Hyperspectral optical fiber refractive index measurement spanning 2.5 octaves

Andrew D. Yablon*[a], Jayesh Jasapara[a]
[a]Interfiber Analysis, LLC, 26 Ridgewood Drive, Livingston, NJ, USA 07039-3120

ABSTRACT

Optical fiber refractive index profiles were measured across a 2.5 octave wavelength range (from 375 nm to 2100 nm) using a single phase-shifting interferometer. This spectral range is more than a factor of 2 larger than previously reported multi-wavelength interferometers, and includes the pump and amplification bands of Er-doped, Yb-doped, Er:Yb-doped, and Tm-doped fibers. The apparatus can measure the material dispersion in a spatially-resolved manner that permits more accurate prediction of the fiber's waveguide properties. The measurement wavelength can be tailored to optimize the beneficial or deleterious effects of material dispersion, optical resolution, and interferometric phase ambiguities.

Keywords: Optical fiber characterization, refractive index measurement, optical fiber refractive index profiling

1. INTRODUCTION

The optical performance of an optical fiber is primarily determined by its refractive index profile, which in turn, depends upon the operating wavelength. While various methods for measuring fiber refractive index profiles have been developed over many decades[1-3], transverse interferometry is particularly well-suited to this task because of the ease with which it can be applied across a multiplicity of measurement wavelengths[1,4-6]. Optical fiber refractive index profiles are traditionally measured at, or near, 632.8 nm, partly because that is a common wavelength for fiber preform measurements and because visible wavelengths provide excellent spatial resolution. However, high-power optical fiber lasers and amplifiers are often operated almost 1 octave away, near 1060 nm. Furthermore, the 1550 nm telecommunications window and operating wavelengths even as long as 2.1 microns have recently grown in popularity and significance[7]. With this wavelength diversity in mind, the potential benefits of a wavelength-agile refractive index measurement apparatus are immediately clear. In this paper we describe a hyperspectral refractive index measurement apparatus based on transverse interferometry that spans from 375 nm in the ultraviolet (UV) to 2.1 microns in the short-wavelength infrared (SWIR), about 2.5 octaves.

Measuring the refractive index across a broad bandwidth offers several advantages. Firstly, the numerical apertures (NA) of certain fibers can vary strongly with wavelength. Such behavior has been observed[4,5] for high-NA rare-earth doped fibers, photosensitive fibers, as well as graded-index multimode fibers. These variations are typically weaker in the infrared but are concentrated in the ultraviolet (UV) or visible wavelengths because of their proximity to optical resonances. Secondly, a multi-wavelength optical fiber index profiler permits the material dispersion to be be measured in a spatially-resolved manner. The relative dopant levels in an optical fiber can be inferred from the measured spectral dependence of the refractive index, as was done in Fig. 3. Furthermore, different wavelength bands can elucidate different features of the fiber-under-test (FUT). For example, shorter measurement wavelengths offer inherently finer spatial resolution. Longer measurement wavelengths can be attractive when the fiber contains abrupt boundaries between substantially dissimilar regions that induce interferometric phase ambiguities, as is the case for fibers containing large-diameter highly-down-doped stress rods (see Fig. 4).

2. EXPERIMENTAL APPARATUS

The experimental apparatus was a Mach-Zehnder interferometer including a sample and reference optical path as shown in Figure 1. A Mach-Zehnder interferometer inherently offers two input ports and two output ports, making it easy to multiplex different optical sources and detectors. It is worth noting that if both input ports contain substantially overlapping illumination wavelengths, no fringes will be produced by the interferometer in the overlapping bands and therefore complementary stop-band filters must be used to segregate the illumination bands if overlapping optical sources are used simultaneously.

Fiber Lasers X: Technology, Systems, and Applications, edited by Sami T. Hendow, Proc. of SPIE
Vol. 8601, 86011V · © 2013 SPIE · CCC code: 0277-786X/13/$18 · doi: 10.1117/12.2000311

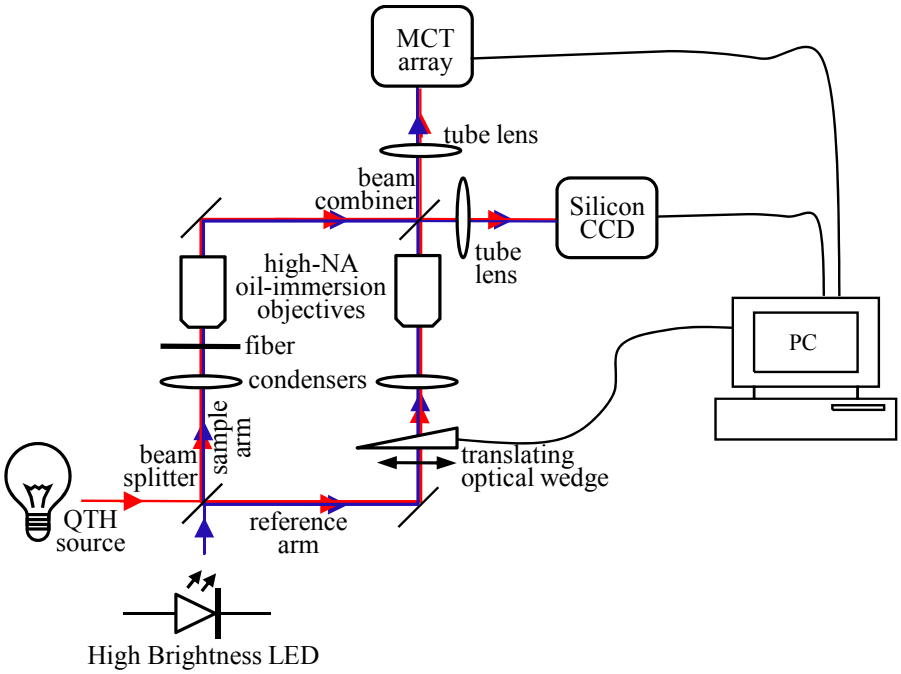

Figure 1. Schematic diagram of Mach-Zehnder interferometer apparatus. The fiber is held by a 4-axis computer controlled stage imposing x, y, and z translation along with rotation about its axis (not shown). MCT array refers to the Mercury-Cadmium-Tellurium imaging detector array. CCD is a silicon charge-coupled-device imaging detector array. LED is a high-power light-emitting-diode. QTH refers to the Quartz-Tungsten-Halogen optical source. High- NA refers to high numerical aperture.

A Quartz-Tungsten-Halogen (QTH) lamp was the primary illumination source in the visible and IR, whereas a high-brightness light-emitting-diode (LED) provided illumination at visible and UV wavelengths. Cut-off or cut-on interference filters were used to isolate different regions of the broad spectrum as necessary. It is important to note that no laser was used for illumination; instead the illumination was completely incoherent, both spatially and temporally.

A conventional room temperature 2/3" format charge-coupled-device (CCD) camera was used as the detector for signals from 370 nm up to 1000 nm. The pixel size of this megapixel detector is about 6.5 microns, and with an effective tube/objective lens magnification of about 35×, each silicon pixel corresponded to about 0.185 microns of distance in the FUT. A thermoelectric (TEC) cooled Mercury-Cadmium-Telluride (MCT, also known as HgCdTe) array detector was used to detect the complementary SWIR illumination, from about 900 nm to about 2100 nm. An important advantage of the MCT detector technology is that its spectral sensitivity increases with increasing wavelength thereby complementing the QTH source whose emission declines with wavelength over this band. The MCT pixel size in this ~80,000 pixel array was about 30 microns, and with an effective tube/objective lens magnification of about 40×, each pixel corresponded to about 0.74 microns of distance in the FUT. While the 0.74 microns/pixel scaling may appear coarse at first glance, this dimension is still much shorter than the wavelengths detected by this array.

In principle, data across the entire spectrum could be acquired simultaneously, but it was found that superior results were achieved by measuring sequentially in separate illumination bands. The operating band of the beam splitter and beam combiner is much broader than the bandwidth of optical correction for the objective lenses. In particular, the optimum focus position of the high-NA oil-immersion objective lenses was found to vary slightly across the band necessitating focal adjustments between the UV/visible and the IR.

The fiber-under-test (FUT) was held by a 4-axis chuck (not shown in Fig. 1) such that it was immersed in refractive index matching oil. The FUT could be scanned across its length, for example to probe axial refractive index variations in a taper or near a fusion splice. The FUT could also be rotated with respect to the apparatus, for example to produce 2-dimensional tomographic data as shown in Fig. 4.

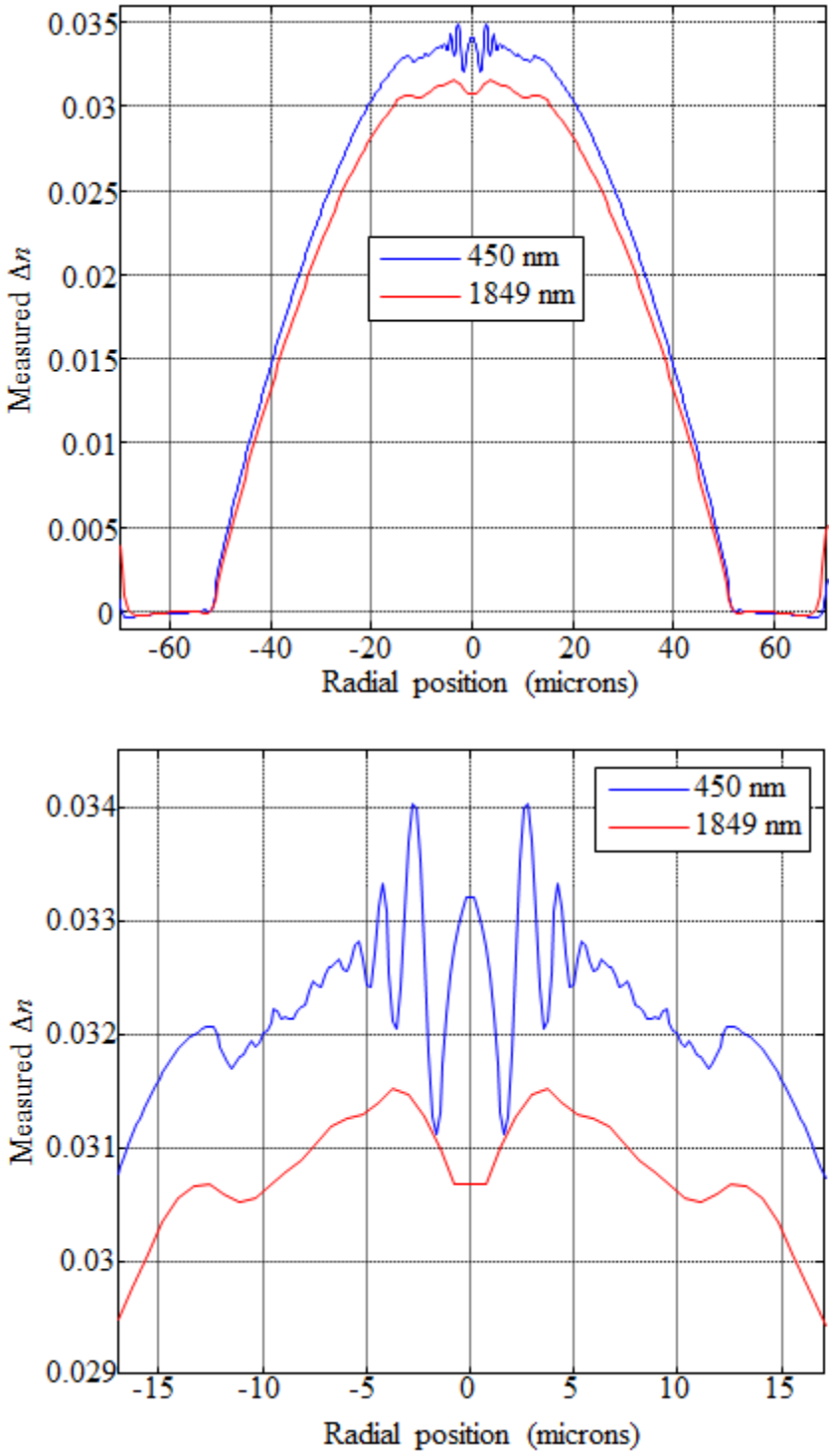

Figure 2. Refractive index profiles measured at two diverse wavelengths on a graded-index multi-mode silica optical fiber. The lower plot is a zoomed-in view of the upper plot. The undulations in the core evident at 450 nm are a real vestige of the layer-by-layer fiber manufacturing process. It is clear that shorter optical wavelengths yield finer spatial resolution. The traces have been adjusted in the Δn axis so that silica cladding Δn is zero. The uncertainty in the refractive index measurement is on the order of +/- 0.0001.

3. RESULTS

Figure 2 shows representative refractive index profile plots obtained on a 100 µm core diameter 140 µm cladding diameter silica graded-index multimode (GI-MMF) fiber. The lower plot is a zoomed-in view of the upper plot. The core composition of this fiber is not known, but presumed to be primarily Germania-doped. The vertical axis in Figure 2 is in units of Δn but both traces have been vertically adjusted to ensure that the cladding is set to a Δn of zero, thereby highlighting the substantial difference in the core Δn, and hence the fiber's NA, at the two disparate wavelengths. The sub-micron details seen in the center of the core at 450 nm are a real vestige of the layer-wise preform manufacturing process. The spatial resolution at 450 nm is clearly finer than the resolution at 1849 nm. The weak curvature in the silica cladding refractive index is a real feature that is characteristic of such fibers and is associated with stresses and strains frozen into the fiber[8].

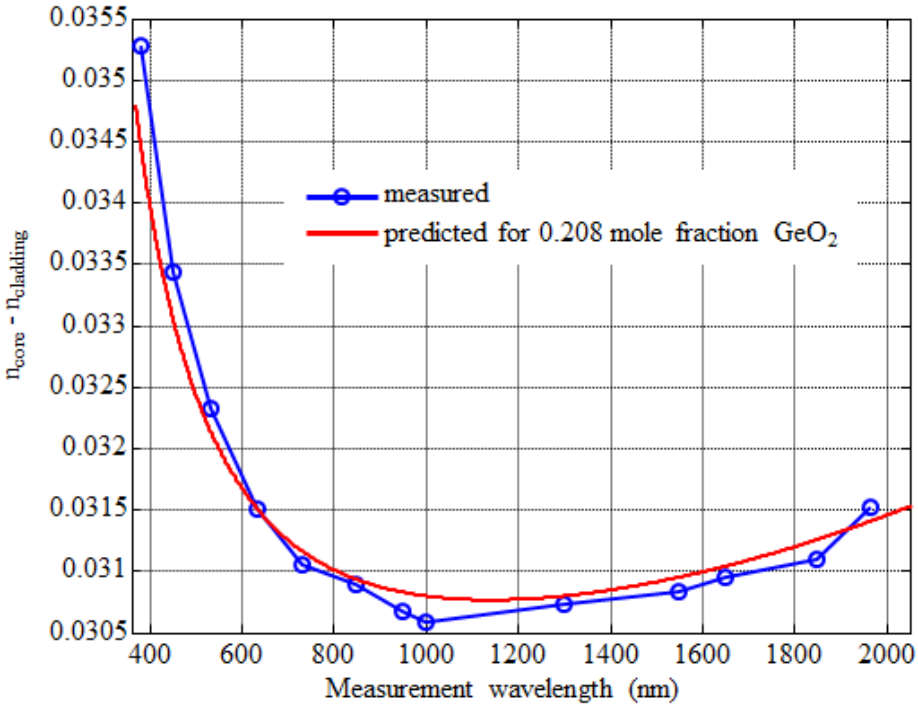

Figure 3. Variation of core-to-clad refractive index difference as a function of measurement wavelength for a graded-index multi-mode silica optical fiber. The predicted data (red) is based on Fleming[9] assuming a Germania mole fraction of about 21% in silica by mass that was chosen based on its close agreement with the measured data.

The average refractive index difference between the core and the cladding (n_{core}-$n_{cladding}$) is depicted in Fig. 3 as a function of wavelength. The data in Fig. 3 is substantially cleaner and spans a much broader wavelength range than previously published data in the references[4,5]. The best fit between measured and predicted data from Fleming[9] was obtained for a mole-fraction of 0.208 of GeO_2 in silica. To our knowledge, the experimental data in Fig. 3 is the first measurement of the refractive index difference between core and cladding of a Ge-doped fiber or preform in the wavelength range of 1000 nm to 2000 nm. This data confirms Fleming's conjecture[9] that the refractive index difference between core and cladding, and hence the fiber's numerical aperture, actually does *increase* over this wavelength range in Ge-doped graded-index multimode fibers. The discrepancy between the measured and predicted data can be partly attributed to the refractive index measurement uncertainty, which is estimated to be on the order of +/- 0.0001. Furthermore, the precise chemical composition of both core and cladding are not known, and other trace dopants, such as chlorine, may be present in addition to Germania.

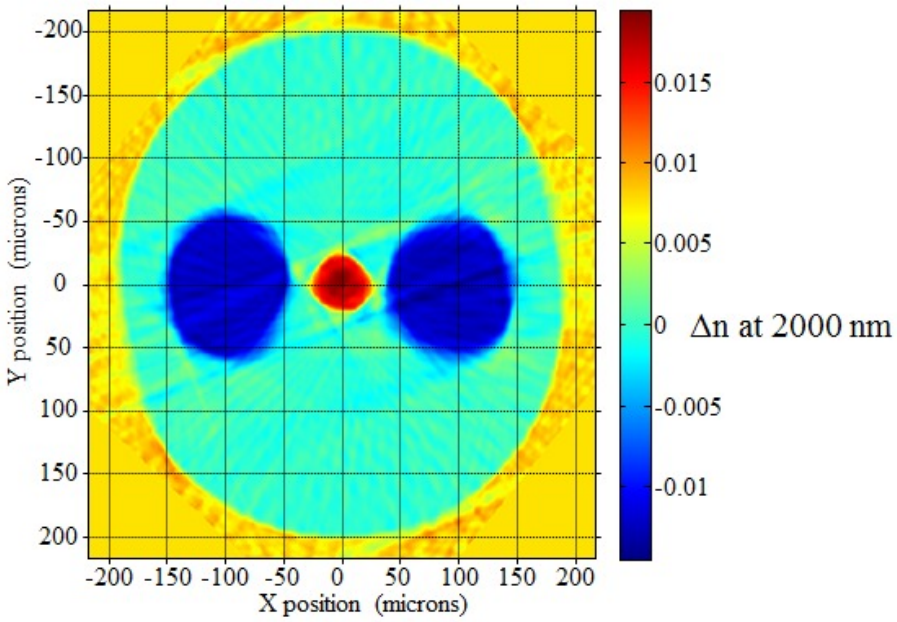

Figure 4. Two-dimensional cross section of Tm-doped polarization maintaining (PM) fiber at 2000 nm. The refractive index is provided in false color. The core asymmetry seen in this measurement is a real property of this fiber. Note also the slight ovality of the cladding shape.

Figure 4 shows a 2-dimensional refractive index map measured on a Tm-doped amplifier fiber containing a pedestal surrounding a rare-earth doped core. The asymmetries evident in the core are not measurement artifacts. The geometry of the presumably boron-doped stress rods is clear from the data. A small amount of cladding ovality is also evident in the data.

4. CONCLUSIONS

A Mach-Zehnder interferometer apparatus for measuring the refractive index of optical fibers at wavelengths from the UV to the SWIR has been described. This instruments permits optical fibers to be characterized in their operating bands, as well as at wavelengths where other benefits, such as superior spatial resolution, can be achieved. These capabilities are particularly attractive for characterizing large-diameter high-power optical fibers designed to operate near 1550 nm or 2 μm wavelength.

REFERENCES

[1] Yablon, A., “Recent Progress in Optical Fiber Refractive Index Profiling”, OFC/NFOEC, (Optical Society of America) paper OMF1 (2011).
[2] Marcuse, D., [Principles of Optical Fiber Measurements] Academic Press, New York, 1981.
[3] Raine, K. W., Baines, J. G. N, and Putland, D. E. “Refractive Index Profiling – State of the Art,” IEEE J Lightwave Technol 7(8), 1162-1169 (1989).
[4] Yablon, A., "Multiwavelength optical fiber refractive index profiling," Proc. SPIE 7580, (2010).
[5] Yablon, A., “Multi-Wavelength Optical Fiber Refractive Index Profiling by Spatially Resolved Fourier Transform Spectroscopy,” IEEE J. Lightwave Technol. 28(4), 360-364 (2010).
[6] Yablon, A. D., “New transverse techniques for characterizing high-power optical fibers,” Optical Eng. 50(11), 111603-1 – 11603-6 (2011).

[7] Richardson, D. J., Nilsson, J., and Clarkson, W. A. “High power fiber lasers: current statusand future perspectives,” J. Opt. Soc. Am. B 27(11) B63-B91 (2010).
[8] Yablon, A. D., “Optical and Mechanical Effects of Frozen-in Stresses and Strains in Optical Fibers,” IEEE J. Sel. Topics Quantum Electron. 10(2), 300-311 (2004).
[9] Fleming, J. W. “Dispersion in GeO_2-SiO_2 glasses,” Appl. Opt. 23(24), 4486-4493, (1984).